SUPERCELLS OF THE SERRANIAS DEL BURRO (MEXICO)

Roger Edwards[1]
Storm Prediction Center, Norman, OK

1. INTRODUCTION and BACKGROUND

The Serranías del Burro (SdB) of northern Coahuila comprise a northern lobe of the Sierra Madre Oriental mountains that dominate much of northeastern and central Mexico. Topographic slopes extend from the SdB to the Rio Grande, along the Texas border (Fig. 1, next page). Mexican relief is strong, with elevations from nearly 3 km in the loftiest SdB to ~50 m in portions of the Rio Grande valley. The SdB is closer to the open Gulf of Mexico (~500 km) than any portion of the U.S. Great Plains.

Since the advent of real-time satellite imagery in the early 1970s, forecasters at the Storm Prediction Center (SPC) and its predecessors have recognized the SdB as a frequent focus for cumulonimbi -- many quite large and long-lived, such that the highest of SdB was nicknamed "magic mountain" and "old faithful" (Weiss, personal communication). Some SdB thunderstorms were observed to last for hours with visible overshooting tops and/or large areas of cold cloud tops in infrared imagery. Forecasters sometimes noticed satellite signatures on SdB storms known to be characteristic of tornadic supercells in the U.S. (e.g. Purdom 1993).

Since the Laughlin Air Force Base (KDFX) WSR-88D unit was commissioned in July, 1994 (NWS-ROC, 2006), storms forming in the Serranías del Burro have been sampled frequently by that radar. Some exhibited signatures common to their supercellular counterparts in the Great Plains, including reflectivity hook-echoes and deep, intense mesocyclones. An SdB supercell sometimes will cross the Rio Grande, producing hail, damaging wind and tornadoes on the American side.

An extreme example formed in the SdB at ~03 UTC, 22 March 2000, apparently peaking in intensity in Mexico *before* producing two tornadoes (damage rated F1 and F0), and 2.5 inch hail in Val Verde County TX (NCDC 2000). Over Coahuila, this storm had at least 100 kt (50 m s^{-1}) gate-to-gate shear in 0.5^O deg elevation storm-relative motion (SRM) data from KDFX (not shown). The SRM peak occurred shortly before and during the appearance of a possible tornadic debris signature in the hook echo (Fig. 3). The signature bore striking similarities to the debris "knobs" associated with Oklahoma tornadoes producing F3 damage (Brown et al. 2005) and F5 damage (Burgess et al. 2002). This indicates that a significant tornado may have hit a remote part of Coahuila containing both bare ground and scrub brush -- but few, if any, permanent structures (based on high resolution GoogleEarth satellite imagery, not shown) -- and that any lofted debris was largely vegetative or geophysical in origin.

A unique overlap of traits makes the SdB area suitable for initiation and support of supercells: the area's elevated terrain (Fig. 1b-c), proximity to often richly moist boundary layer of the western Gulf of Mexico, and its latitudinal positioning beneath subtropical middle and upper tropospheric jets that contribute to deep-tropospheric vertical wind shear.

Herein, a limited sample of these supercell events will be summarized and analyzed, both individually and in composite, covering a 2.5 year period.

2. EVENT DATA and DESCRIPTIONS

From 2004-2006, 13 supercells were documented within the SdB or adjacent foothills. The same radar-based strength and persistence criteria defined a supercell as in Thompson et al. (2003, hereafter T03). For storms initiating outside KDFX range, such as 28 May 2005, satellite imagery was used to determine locations until the storms could be followed using the radar. Infrared and moisture channel satellite imagery were incorporated, in combination with subjectively analyzed, mandatory-level upper-air charts, to determine the ambient synoptic regimes for each event, summarized in Table 1 and briefly discussed in Section 3.1.

Among the observed and RUC (Benjamin et al. 2004) 00-h soundings available for each event, a single most-representative inflow sounding was selected for analysis and for use in compositing. This choice was subjective, based on distance to the storm, elevation, character of surface observations (eliminating, for example, soundings with no CAPE and those on the stable side of drylines or other boundaries from the storm itself). Where either the 00 UTC RUC or observed sounding from DRT could be considered most-representative, the observed sounding was chosen. Otherwise, a RUC sounding was used if it was closer in space and time to the storm than were the 00 UTC observed soundings. This approach was based on the findings of T03, who illustrated that RUC soundings may serve as adequate proxies in the absence of observed RAOB data for supercell situations.

3. ANALYSES and PRELIMINARY FINDINGS

3.1. Synoptic to mesoβ–scale settings

Middle-upper tropospheric patterns (Table 1) were characterized by SW or WSW flow, associated with synoptic scale troughs over western or central North America. Considerable wind speed variability aloft was evident from case to case. Slower and more deviant

---

[1] *Corresponding author address:* Roger Edwards, Storm Prediction Center, National Weather Center, 120 Boren Blvd #2300, Norman, OK 73069; E-mail: roger.edwards@noaa.gov
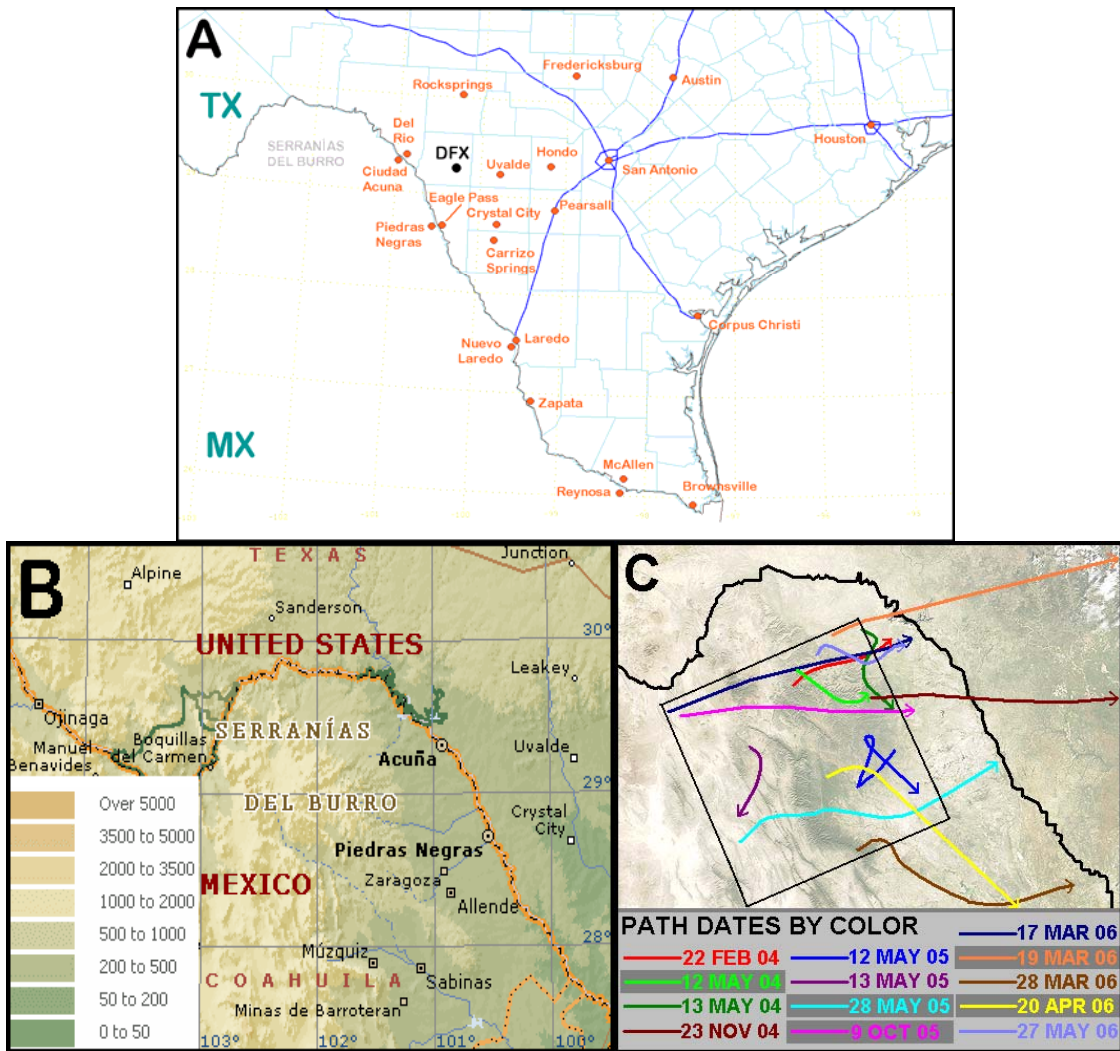
Figure 1. Reference maps of the Serranías del Burro region: **a)** Political, with international border and U.S. County outlines. Cities and select major towns are in orange, U.S. interstate highways are blue; **b)** Relief/political blend, courtesy MSN Encarta. Elevations are color coded in m MSL; **c)** Color-coded paths for the reflectivity centroid of each supercell in Table 1, overlaid on an enhanced MODIS visible satellite image (courtesy NASA). Square is 100 nm (161 km) on a side and encloses all storm genesis points.
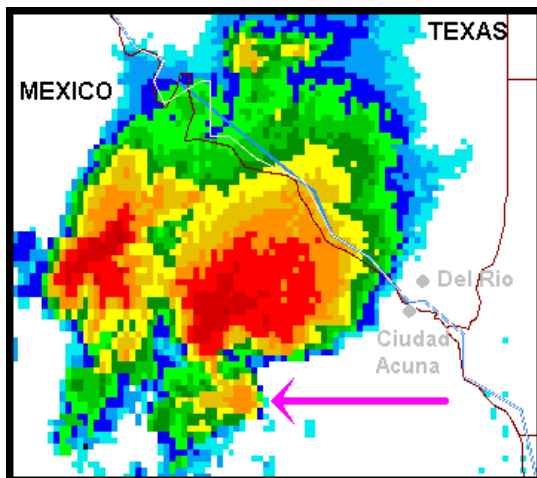

Figure 2. Base reflectivity image from KDFX, 0.5^O elevation angle, 22 March 2000, 0540 UTC. Arrow points toward hook echo and possible tornadic debris "knob" signature.
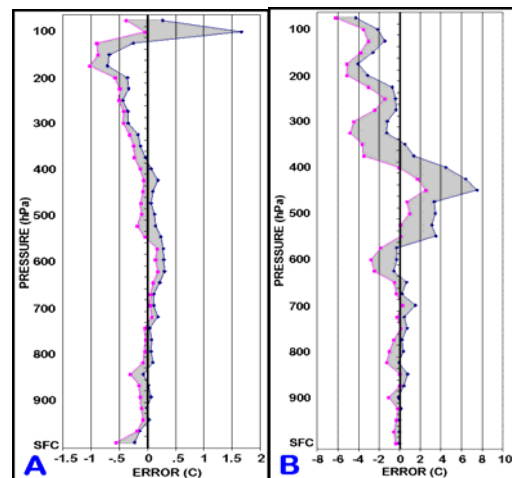
Figure 3. Vertical profiles of 95% confidence intervals for ^{O}C errors in **a)** temperature and **b)** dew point, for 00 UTC RUC comparison soundings at DRT (described in the text).

Table 1. List of collected SdB supercell events. Bold rows denote supercells that moved into the U.S. as such. Pattern summary is based on examination of synoptic scale satellite imagery and subjective analysis of mandatory level charts at 250, 500 and 700 hPa. "STJ" denotes subtropical jet (250 hPa). Most representative sounding was selected subjectively from observed data at Del Rio, TX (DRT) or Corpus Christi, TX (CRP), or Rapid Update Cycle (RUC) proximity data from DRT, CRP, Laredo, TX (LRD) or El Cimarron, Mexico (G#3) in the southwestern SdB. Life span is that of the entire discrete echo associated with the supercell, not the amount of time of supercell structure. Motion denotes the vector from which the mature phase supercell moved.

EVENT DATE (UTC)	GENERALIZED MIDDLE-UPPER TROPOSPHERIC PATTERN SUMMARY	MOST REP. SOUNDING	LIFE SPAN (h)	MOTION (dir/spd in kt)
22 Feb 2004	SW flow, STJ max ≥140 kt overhead, shortwave trough over Chihuahua, neg. tilt synoptic trough over coastal CA & Baja	OBS (DRT) 23/00 UTC	2.3	255/20
12 May 2004	Difluent SW flow, N edge of STJ, synoptic trough from western MT past Baja spur, possible weak perturbation over western Coahuila	RUC (DRT) 12/23 UTC	3.4	305/08
13 May 2004	Difluent SW flow, neutral tilt synoptic trough Saskatchewan to eastern Chihuahua, no STJ nearby	RUC (DRT) 13/21 UTC	3.7	000/13
23 Nov 2004	**SW flow, NW edge of ≥ 111 kt STJ max, high amplitude & progressive trough western KS to northern Chihuahua to southern Baja**	**OBS (CRP) 24/00 UTC**	**6.0**	**270/35**
12 May 2005	Weakly difluent WSW flow, synoptic low eastern MT with pos. tilt trough SW past Baja spur, STJ S of area	RUC (DRT) 13/03 UTC	6.7	Stationary
13 May 2005	WSW flow, northern edge of subtropical upper jet max, synoptic trough Manitoba to SE NM, weak shortwave perturbations over northern Chihuahua and central Baja	RUC (G#3) 13/21 UTC	4.2	020/10
28 May 2005	SW flow, pos. tilt trough NW KS to southern Baja, embedded weak 500 hPa low over SE NM, 250 hPa cyclone center between DRT-Midland, N edge of STJ	RUC (G#3) 28/20 UTC	5.8	265/21
9 Oct 2005	SW flow, STJ max ≥ 75 kt overhead, synoptic low over SW CO with trough to west-central Mexican Pacific coast, weak shortwave trough over Chihuahua	RUC (G#3) 10/02 UTC	3.6	270/28
17 Mar 2006	Difluent SW flow, ~50 kt STJ flow SE of ~90 kt max in SE NM, high-amplitude synoptic trough WA to central CA to offshore Baja	RUC (G#3) 18/01 UTC	6.8	255/18
19 Mar 2006	**SW flow, STJ 108 kt at DRT and 120 kt at El Paso, deep synoptic low northern UT, strong shortwave trough southern AZ & Sonora, possible weak shortwave trough southern Chihuahua**	**OBS (DRT) 20/00 UTC**	**7.5**	**250/29**
28 Mar 2006	Difluent WSW flow, right-entrance region of STJ max (124 kt over SE TX, 65 kt at DRT), synoptic low just offshore CA/OR border with neg. tilted trough offshore southern CA & northern Baja, shortwave trough over Chihuahua	RUC (DRT) 29/01 UTC	5.8	295/15
20 Apr 2006	WSW flow, STJ max ≥76 kt overhead, synoptic low central MN, shortwave trough northern TX panhandle to NW Coahuila	RUC (LRD) 21/04 UTC	6.1	320/20
27 May 2006	Weakly difluent SW flow, broad/50-55 kt STJ overhead and S of area, synoptic low southern ID with trough to NW Baja	OBS (DRT) 28/00 UTC	3.1	280/09
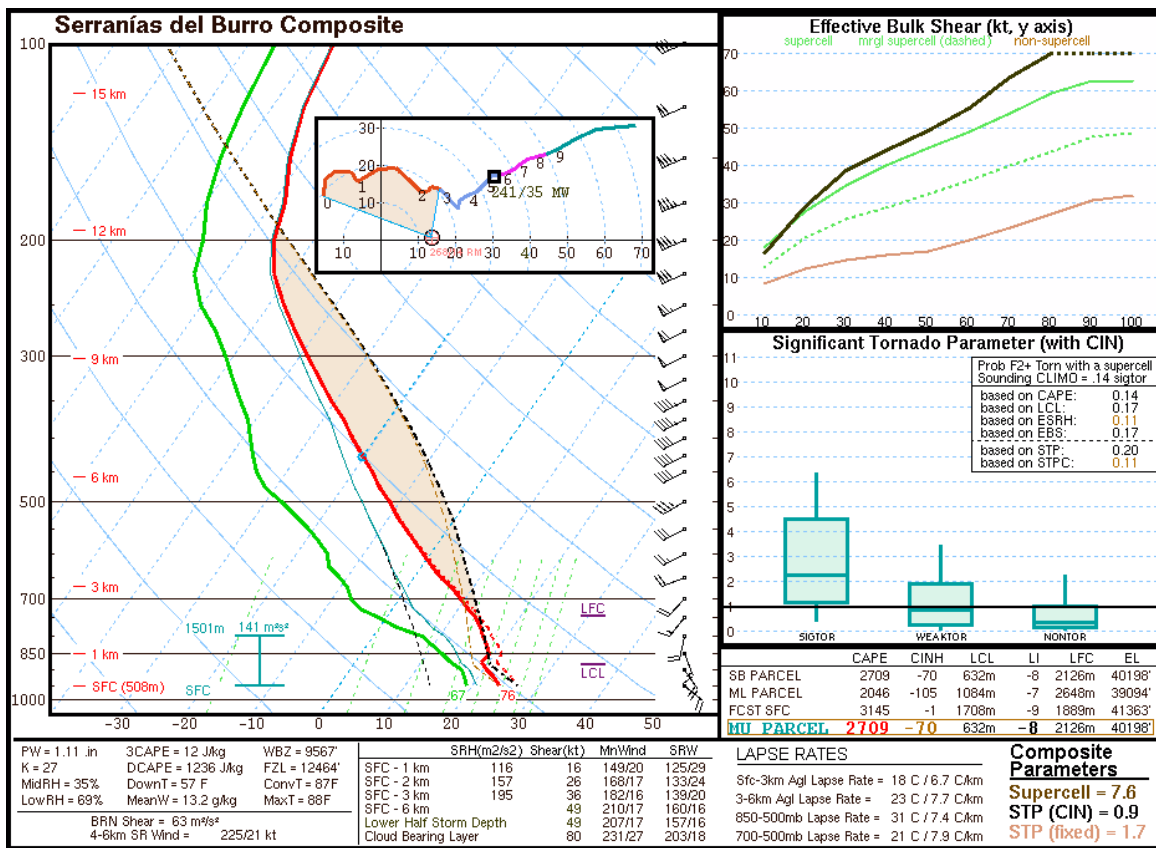
Figure 4. .Skew-t and inset hodograph of the 13-sounding SdB composite (see text). Hodograph is labeled every km AGL. Tan shading represents CAPE (storm-relative helicity or SRH) on the sounding (hodograph). Commonly used calculations and derived parameters are given in the text tables. Composite and effective bulk parameters at right are from Thompson et al. (2003 and 2006). Effective bulk shear and significant tornado parameter (STP) are in black lines, for comparison to climatological median and 90th percentile ranges on the x-y and box and whiskers diagrams, respectively [based on the RUC soundings of Thompson et al. (2006)]. Inset probabilities for STP are based on set intervals of values from T06 data for 100 hPa mixed-layer CAPE (MLCAPE, ~1000 J kg^{-1}), ML lifted condensation level (~250 m), effective SRH (~50-100 m^2 s^{-2}), ESHEAR (10 kt), and STP (~1).

(rightward) moving storms well within Mexico occurred in weaker winds aloft than those crossing the border or with long paths ending just west of the Rio Grande. The two that crossed the river were in early spring (Mar.) and late fall (Nov.) under or very near 250 hPa and 500 hPa jet maxima >100 kt (50 m s^{-1}) and 50-75 kt (25-38 m s^{-1}) respectively. In seven cases, shortwave troughs were evident upstream over northwestern Mexico – primarily identified in moisture channel imagery, given the lack of observed sounding data.

In low levels, E to SE surface winds veered to S around 850 hPa, yielding strong low level directional shear. In ten cases, a baroclinic zone (front or outflow boundary) was analyzed over portions of the SdB region, only one of which (23 Nov. 2004) was a cold front. Most fronts in the vicinity of SdB supercells were stationary or warm in nature, with surface dew points increasing with time amidst E to SE winds. Three supercells were clearly in warm sectors, each characterized by increasing surface moisture with time and with seaward extent. Lack of dense Mexican surface observations lends uncertainty about whether the storms initiated *on* the boundaries, but it is clear that supercells often are associated with at least the nearby interaction of a baroclinic zone and the SdB. In all 13 cases, orographic ascent was inferred

over the eastern SdB, either from near-frontal easterlies or relatively backed warm-sector flow.

3.2. *RUC comparison soundings*

The T03 premise of RUC soundings as proxies for observed soundings in U.S. supercell environments was retested here to assess regional validity. During each event, observed and RUC analysis soundings from DRT were gathered at 00 UTC and compared to gauge model error, for a total of 13 comparisons. Because significant-level data did not match levels from RUC to observed sounding, data above the surface were interpolated to identical 25 hPa intervals as in T03, followed by error computations thereon. For mandatory levels (e.g., 850, 700, 500 hPa, etc.), the values could be compared directly without significant-level interpolation. Overall results concur with T03 in that RUC soundings are viable proxies.

RUC thermal soundings tended to be slightly cool at the surface with a mean error of -0.4°C. This *may* be related to a consistent model overestimate of ground height at DRT (below). This coolness eased considerably (-0.16°C) at the first level aloft (975 hPa).

Mean absolute errors (MAE) for temperature were less than 1^{O}C from the surface through 150 hPa. Except for slight coolness in the boundary layer and upper troposphere, vertical profiles of 95% confidence intervals of thermal errors (Fig. 3a, analogous to Fig. 2 in T03) generally were at or below the 0.5^{O}C accuracy of radiosondes (NOAA 2006). Dew point MAE was under 2^{O}C in lower-middle levels (surface through 650 hPa). The model had its most trouble ascertaining moisture in middle-upper levels, with MAE ranging from 3.3-6.8^{O}C in the 550-300 hPa layer. Dew point errors were smaller and closer to zero at the 95% confidence interval than thermal errors (Fig. 3) from surface to the 600-650 hPa layer.

The mean RUC height error at its model surface was 33.4 m, an order of magnitude larger than at any level aloft (e.g., 6.1 m at 500 hPa). This indicates a systematic RUC overestimate of ground elevation at the DRT site; indeed, examination of individual errors showed no underestimates. Through most of the troposphere, however, height errors were small.

RUC winds averaged within 2 kt (1 m s^{-1}) of observed speeds through the lower to middle levels (beneath 400 hPa). RUC winds were somewhat too weak in upper levels (mean error -4.2 kt at 300 and 275 hPa). Error plots at the 95% confidence interval remained within 0.5 kt (0.25 m s^{-1}) of zero error from the surface through 300 hPa (not shown). On average, RUC surface winds were slightly too backed (-13°), but directional errors tended to dampen with height through the midtroposphere (i.e., MAE of 3.7^O at 500 hPa).

3.3. *Event composite soundings*

Composite soundings were prepared using four observed and nine RUC soundings deemed most-representative. Identical interpolation was applied as in the comparison soundings, then averaged 25 hPa intervals to derive the composites. Five cases involved high elevation soundings in the SdB whose greatest interpolative pressure is 850 hPa; so only eight soundings contained data representative of the Rio Grande valley and adjacent parts of the U.S.

Because of elevation differences in soundings, two composites were assembled. The first (Fig. 4) contains all soundings' data from 850-100 hPa, plus the data from 950-875 hPa averaged from eight Rio Grande soundings. The second (not shown) represents *only* 850-100 hPa data from every case. The former was examined for vertical discontinuities in either thermodynamic or wind profiles near 850 hPa which physically would invalidate the profiles (i.e., superadiabatic lapse rates or sudden wind shifting). Despite the small sample size, the vertical transition in thermodynamic and wind strata near 850 hPa, between the eight-sounding lower levels and the 13-sounding remainder, was relatively smooth. That factor, along with the absence of 950-875 hPa data for the Rio Grande valley in the second and shallower composite, motivated the selection of the deeper composite sounding for emphasis in this study.

Of course, caution is needed with any averaging or compositing of a mere 13 cases. Results may be subject to substantial change after larger sampling. With that caveat in mind, the composite sounding shows a variety of favorable parameters for supercells (listed in Fig. 4, defined in Thompson et al. 2003 and 2006).

4. SUMMARY and DISCUSSION

This paper presents 13 cases of supercells from the Mexican SdB or its foothills, during the period 2004-2006. A few events may have been missed because of unavailable real time data; however, daily basic examination of this area indicates that this sample represents at least a large majority of actual supercell events during this time frame. Storm cases will continue to be accumulated to yield a more robust sample size for various forms of analysis.

The 2.5 year sample implies little about long term trends for supercells. Automated algorithmic processing of historical KDFX data since 1994 should provide a more robust supercellular climatology for the SdB area. Likewise, until Mexican severe weather reports are documented systematically, algorithmic analysis of KDFX velocity vortex signatures (e.g., Jones et al. 2004) and hail detection methods (e.g., Witt et al. 1998 and future dual-polarimetric successors) may be the most reliable way to assess the probability of tornado and hail events, respectively, both in real time and historically. Such an examination also could include either:

1) Presumptive application of U.S. algorithmic climatology showing that ~26% of mesocyclones are tornadic (using the criteria of Trapp et al. 2005); or more intricately,

2) Neural network analyses of nonlinear mesocyclone attributes (Marzban and Stumpf 1996) rooted in U.S. algorithmic correspondences with severe reports. This would yield a series of probabilities for tornadoes and other severe modes on the Mexican side, which may serve as a coarse proxy for the missing climatology of ground truth between the SdB and the Rio Grande.

In the absence of long-term supercell climatology, it is unknown whether the period of this study represents an active, inactive or "normal" rate of supercells for this area. The 13 storms formed within a square 100 nm (161 km) on a side (Fig. 1c), approximating the area of the northwestern quarter of the main body of Oklahoma. Documentation of so many events in this period, combined with anecdotal observations of SPC forecasters over ~30 years, suggests that the SdB region is a prolific spawning ground for supercells, at least as much as any similarly sized (10,000 mi^2 or 25,921 km^2) area in the central U.S. In terms of an ingredients-based framework for severe storms (e.g., Johns and Doswell 1992) this appears to result from the SdB area's uncommon geospatial juxtaposition of

1) Elevated, steeply sloped terrain for *lift*,

2) Close proximity to a rich maritime tropical source of boundary layer *moisture*,

3) Lower-middle level instability in the Mexican plateau's elevated mixed layer, and

4) Enhanced *Vertical shear* related to upslope surface wind component in return flow frontal regimes, and to the SdB position under either the subtropical jet or the southern fringes of cool-season enhancements to upper level flow.

A bimodal seasonal distribution (late winter through mid spring, and to a lesser degree, autumn) of SdB supercells likewise is apparent from this small dataset and from anecdotal observation, but statistical confirmation also awaits longer temporal datasets.

The greatest impediment to meteorological analyses in the SdB is the lack of *in situ* observational data. This is especially encumbering for diagnoses in the afternoon/ evening convective cycle, where 00 UTC rawinsonde launches are rare in Mexico, and where alternative upper air data sources (e.g., radar-derived winds, profilers, and aircraft measurements) also are scant to absent. Until this situation is ameliorated, forecasters in both nations may use KDFX data for critical clues about the environment (i.e., vertical wind profiles), storm-scale processes, and even the possibility of a tornado using both current data and future polarimetric debris detection (e.g., Rhyzhkov et al. 2005). Satellite derived winds also may be useful for diagnosing vertical shear profiles in and upstream from the SdB.

The SdB seems ideal for a collaborative field project involving U.S. and Mexican researchers and their agencies, given its concentration of supercells, the lack of data on their Mexican effects, and the scientific need to understand severe convective initiation and evolution that has fueled the development of projects such as the International H_2O Project (IHOP, after Weckwerth et al. 2004) and Verification of the Origin of Rotation in Tornadoes Experiment (VORTEX, after Rasmussen et al. 1994). Furthermore, precedent exists for such cross-border research cooperation in the form of the Southwest Area Monsoon Project (SWAMP, e.g., Farfán and Zehnder 1994) and the North American Monsoon Experiment (NAME, Higgins et al. 2006). There are few suitable roads evident on various Mexican road maps and in high-resolution GoogleEarth imagery, perhaps compelling a "sit and wait" strategy for mobile mesonets and radars. However, aircraft observation is not so hindered. Also, with cooperation of public and private land owners on both side of the border, fixed mesonet systems may be deployed as part of such a study.

ACKNOWLEDGMENTS

REFERENCES

Benjamin, S.G., and co-authors,, 2004: An hourly assimilation-forecast cycle: The RUC. *Mon. Wea. Rev.*, **132**, 495-518.

Brown, R.A., and co-authors, 2005: Improved detection of severe storms using experimental fine-resolution WSR-88D measurements. *Wea. Forecasting*, **20**, 3-14.

Burgess, D.W., and co-authors, 2002: Radar observations of the 3 May 1999 Oklahoma City tornado. *Wea. Forecasting*, **17**, 456-471.

Higgins, W., and co-authors, 2006: The NAME 2004 field campaign and modeling strategy. *Bull. Amer. Meteor. Soc.*, **87**, 79-94.

Johns, R. H., and C. A. Doswell III, 1992: Severe local storms forecasting. *Wea. Forecasting*, **7**, 588-612.

Jones, T.A., K.M. McGrath, and J.T. Snow, 2004: Association between NSSL Mesocyclone Detection Algorithm-detected vortices and tornadoes. *Wea. Forecasting*, **19**, 872-890.

Farfán, L.M., and J.A. Zehnder, 1994: Moving and stationary mesoscale convective systems over northwest Mexico during the Southwest Area Monsoon Project. *Wea. Forecasting*, **9**, 630-639.

Marzban, C., and G. J. Stumpf, 1996: A neural network for tornado prediction based on Doppler radar-derived attributes. *J. Appl. Meteor.*, **35**, 617–626.

National Climatic Data Center (NCDC), 2000*: Storm Data*, **42**, no. 3, W. Angel, Ed., 172 pp.

National Oceanic and Atmospheric Administration (NOAA), cited 2006: Systems and equipment. Rawinsonde and Pibal Observations, *Federal Meteorological Handbook* No. 3. [Available at http://www.ofcm.gov/fmh3/text/chapter2.htm .]

National Weather Service Radar Operations Center (NWS-ROC), 2006: Site ID Database. Available through http://www.osf.noaa.gov/ssb/srchmain.asp .

Purdom, J.F.W., 1993: Satellite observations of tornadic thunderstorms. *The Tornado: Its Structure, Dynamics, Prediction, and Hazards. A.G.U. Geophys. Monog.*, No. 79, Amer. Geophys. Union, 265-274.

Rasmussen, E.N., and co-authors, 1994: Verification of the Origin of Rotation in Tornadoes Experiment: VORTEX. *Bull. Amer. Meteor. Soc.*, **75**, 1-12.

Rhyzhkov, A.V., T.J. Schuur, D.W. Burgess, and D.S. Zrnic, 2005: Polarimetric tornado detection. *J. Appl. Meteor.*, **44**, 557-570.

Thompson, R.L., R. Edwards, J.A. Hart, K.L. Elmore and P. M. Markowski, 2003: Close proximity soundings within supercell environments obtained from the Rapid Update Cycle. *Wea. Forecasting*, **18**, 1243-1261.

Thompson, R. L., C. M. Mead, and R. Edwards, 2006: Effective storm-relative helicity and bulk shear in supercell thunderstorm environments. Accepted to *Wea. Forecasting*.

Trapp, R.J., G.J. Stumpf, and K.L. Manross, 2005: A reassessment of the percentage of tornadic mesocyclones. *Wea. Forecasting*, **20**, 680-687.

Weckwerth, T.M., and co-authors, 2004: An overview of the International H2O Project (IHOP_2002) and some preliminary highlights. *Bull. Amer. Meteor. Soc.*, **85**, 253-277.

Witt, A., M.D. Eilts, G.J. Stumpf, J.T. Johnson, E.D. Mitchell, and K.W. Thomas, 1998: An enhanced hail detection algorithm for the WSR-88D. *Wea. Forecasting*, **13**, 286-303.